Science Advances
AAAS

Supplementary Materials for

Identification of a targeted ACSL4 inhibitor to treat ferroptosis-related diseases

Qian Huang *et al.*

Corresponding author: Yi Huang, hy527@jiangnan.edu.cn; Fei Gao, gaofei-lx@163.com; Wen Xu, xuwen6779@ustc.edu.cn

Sci. Adv. **10**, eadk1200 (2024)
DOI: 10.1126/sciadv.adk1200

The PDF file includes:

Other Supplementary Material for this manuscript includes the following:

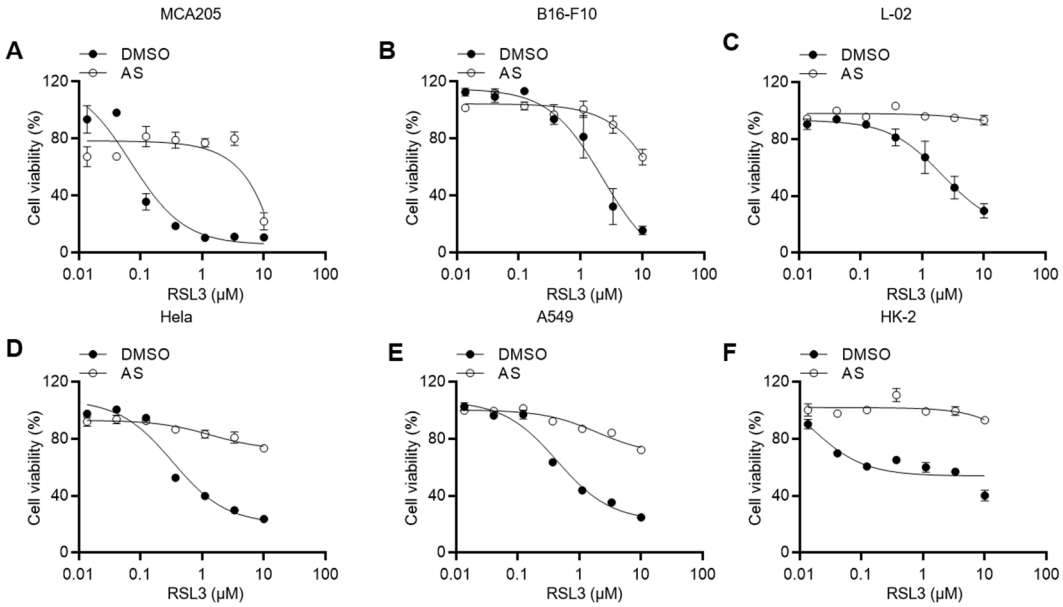

Fig. S1. AS inhibits RSL3-induced ferroptosis in multiple human and murine cells. (A-F) Cell viability analysis of MCA205 (A), B16-F10 (B), L-02 (C), Hela (D), A549 (E) and HK-2 (F) cells pretreated with or without AS for 1 h and then stimulated with different concentrations of RSL3 for 8 h. Data are the mean ± SEM, n = 3 biologically independent experiments.

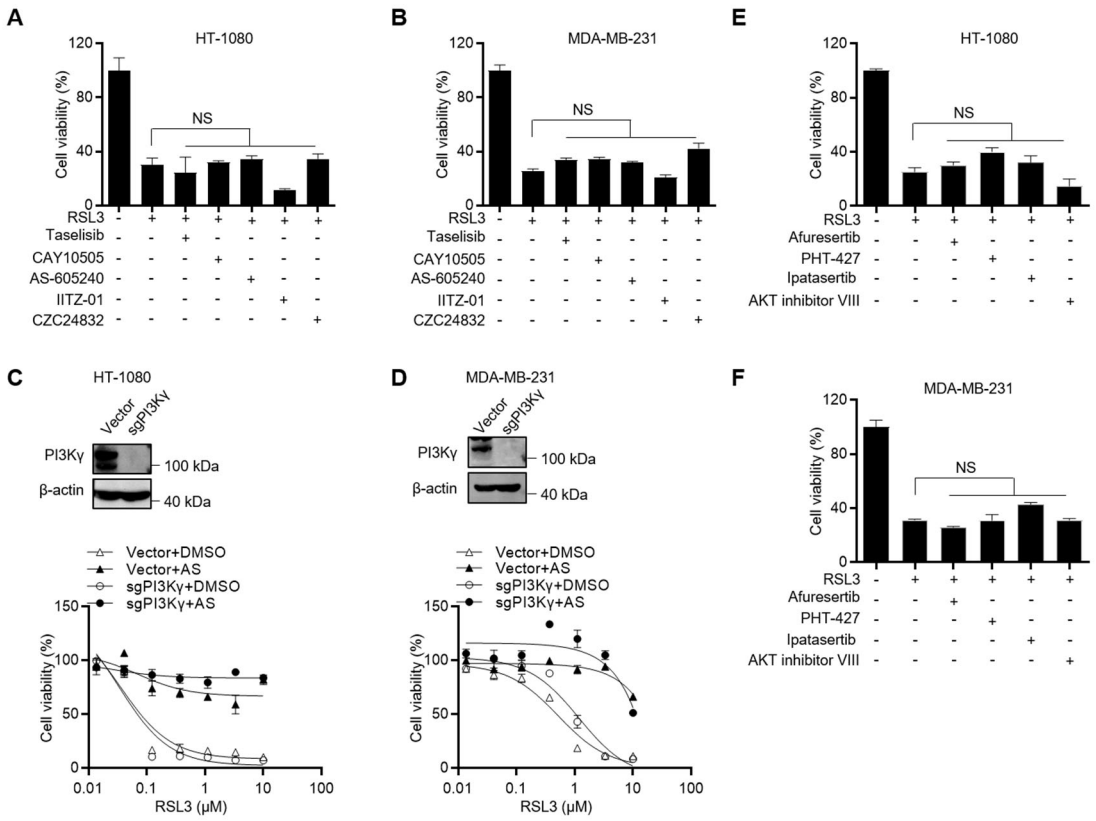

Fig. S2. AS inhibits ferroptosis independent of PI3K/AKT pathway. (A, B) Cell viability analysis of HT-1080 (A) or MDA-MB-231 (B) cells pretreated with 10 μM Taselisib, CAY10505, AS-605240, IITZ-01 and CZC24832 for 1 h and then stimulated with 1 μM RSL3 for 8 h. (C, D) CRISPR-Cas9-generated *PI3Kγ*-knockout HT-1080 cells (C) or MDA-MB-231 cells (D) were treated with AS for 1 h and then stimulated with different concentrations of RSL3. The expression of PI3Kγ was detected by immunoblotting (Above) and the cell viability was detected by CCK-8 assay (Below). (E, F) Cell viability analysis of HT-1080 (E) or MDA-MB-231 (F) cells pretreated with 10 μM Afuresertib, PHT-427, Ipatasertib and AKT inhibitor VIII for 1 h and then stimulated with 1 μM RSL3 for 8 h. Data are the mean ± SEM, n = 3 biologically independent experiments. Statistical analysis was performed using an unpaired two-tailed Student's t-test. NS, $P > 0.05$.

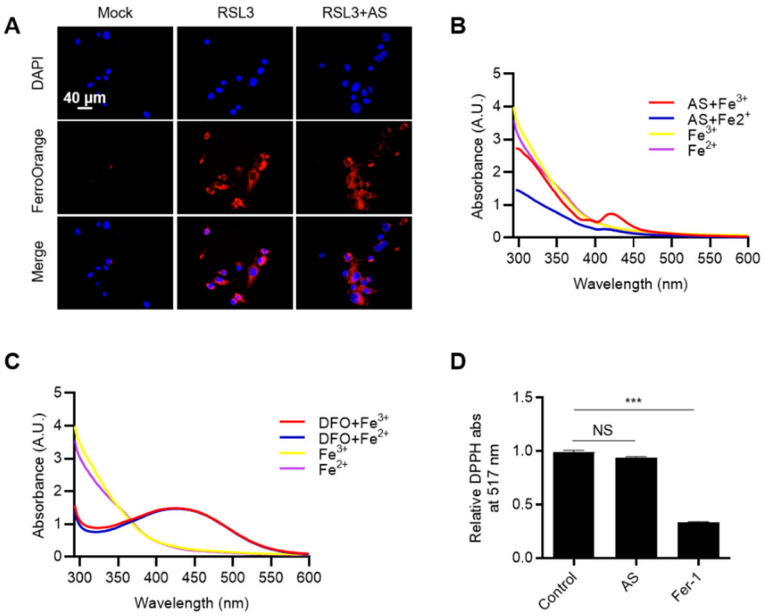

Fig. S3. AS cannot directly chelate iron or scavenge radicals. (A) HT-1080 cells pretreated with AS for 1 h and then stimulated with 1 μM RSL3 for 8 h, and ferrous ion levels were detected by FerroOrange staining. (B, C) UV−vis absorption spectra of DFO and AS in the absence or presence of Fe^{3+} or Fe^{2+}. (D) Cell-free antioxidant potential monitored by changes in the absorbance at 517 nm of the stable radical DPPH. The concentration of all tested compounds was 50 μM. Data are the mean ± SEM. n = 3 biologically independent experiments (D). Statistical analysis was performed using an unpaired two-tailed Student's t-test. NS, $P > 0.05$, ***$P < 0.001$.

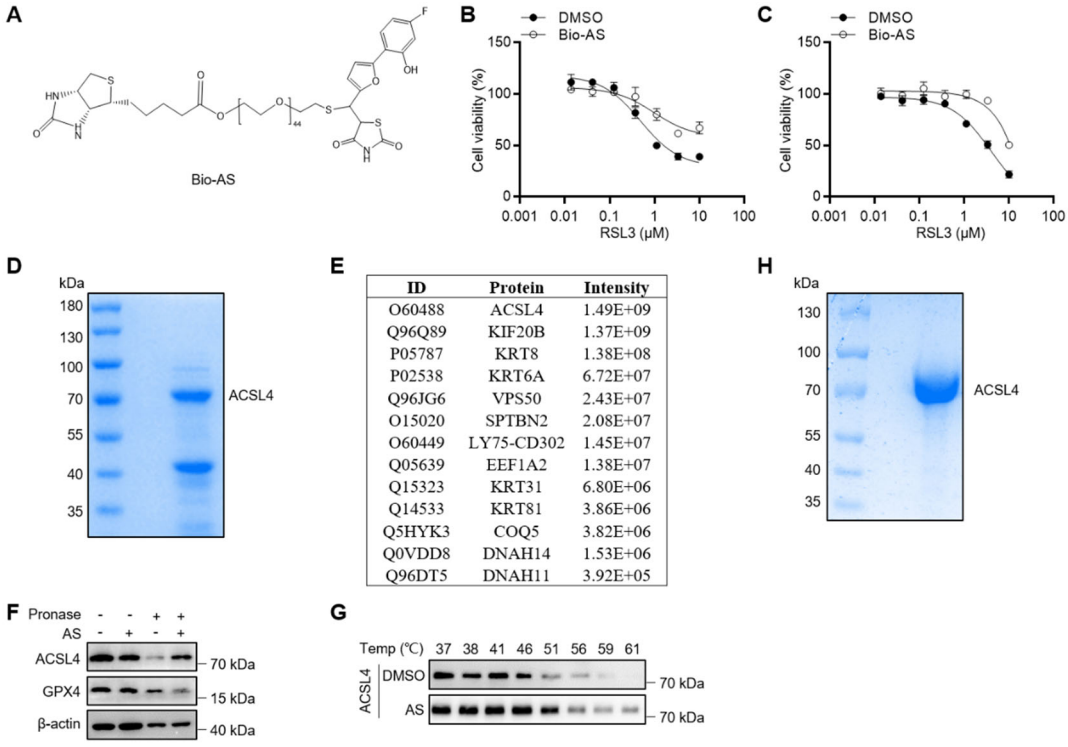

Fig. S4. AS binds to ACSL4. (A) Chemical structure of biotin-tagged AS (Bio-AS). (B, C) Cell viability analysis of HT-1080 (B) or MDA-MB-231 (C) cells pretreated with Bio-AS for 1 h and then stimulated with different concentrations of RSL3 for 8 h. (D) HT-1080 cells treated with free AS or bio-AS, and then the whole cell lysate was pull-down with streptavidin beads. The protein affinity pull-down assay was performed and the precipitated proteins were separated by SDS-PAGE and stained with Coomassie blue. (E) LC-MS/MS analysis the binding proteins of AS. (F) The cell lysates of MDA-MB-231 were incubated with or without AS for 2 h and then treated with 2 μg/ml pronase. The expression of ACSL4 and GPX4 were detected by immunoblotting. (G) The cell lysates of MDA-MB-231 were incubated with or without AS for 2 h and then treated with increasing melting temperature (37-61°C). The expression of ACSL4 was detected by immunoblotting. (H) Coomassie blue staining of recombinant ACSL4 protein. Data are the mean ± SEM, n = 3 biologically independent experiments.

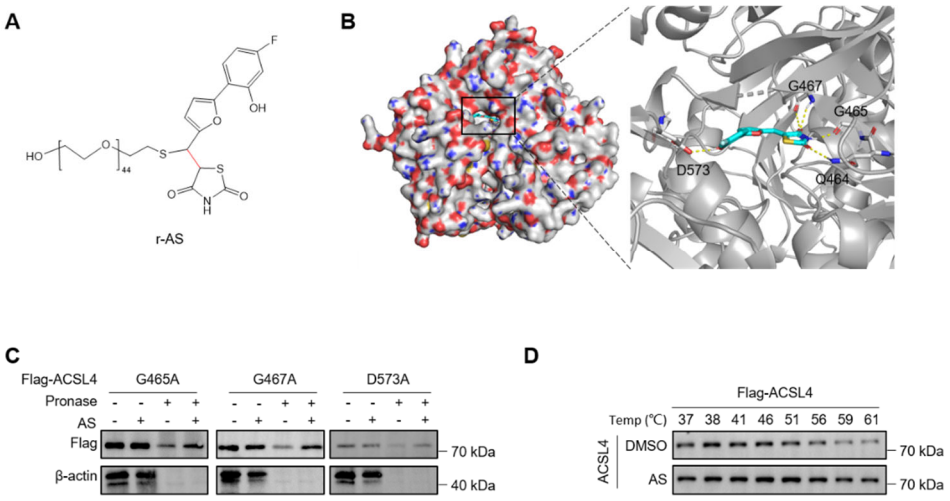

Fig. S5. **Identification of the binding sites of AS and ACSL4.** (A) Chemical structure of r-AS. (B) Docking complex of ACSL4 with AS. AS is shown in sticks and colored light green, ACSL4 is shown in cartoon and colored light gray, key amino acid residues were shown as sticks. (C) The cell lysates of HEK293T overexpressing G465A, G467A or D573A mutant Flag-ACSL4 were incubated with or without AS for 2 h and then treated with different concentrations of pronase. The expression of ACSL4 was detected by immunoblotting. (D) The cell lysates of HEK293T overexpressing WT Flag-ACSL4 were incubated with or without AS for 2 h and then treated with increasing melting temperature (37-61°C). The expression of ACSL4 was detected by immunoblotting.

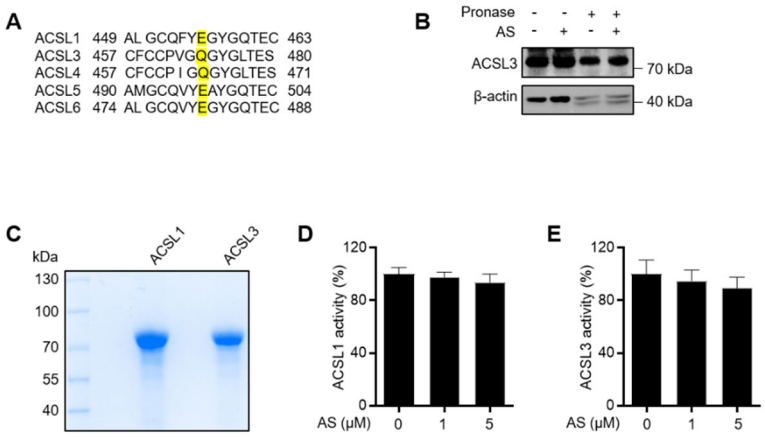

Fig. S6. **AS had no effect on ACSL1 and ACSL3.** (A) Sequence alignments and sequence logos of the labeled motifs and residues are shown for human ACSL1, 3-6. (B) The cell lysates of HT-1080 were incubated with or without AS for 2 h and then treated with pronase. The expression of ACSL3 was detected by immunoblotting. (C) Coomassie blue staining of recombinant ACSL1 and ACSL3 protein. (D, E) Recombinant ACSL1 protein or ACSL3 protein were incubated with different concentrations of AS for 10 min at 37 °C. The enzymatic activity of ACSL1 and ACSL3 were analyzed. Data are the mean ± SEM, n = 3 biologically independent experiments.

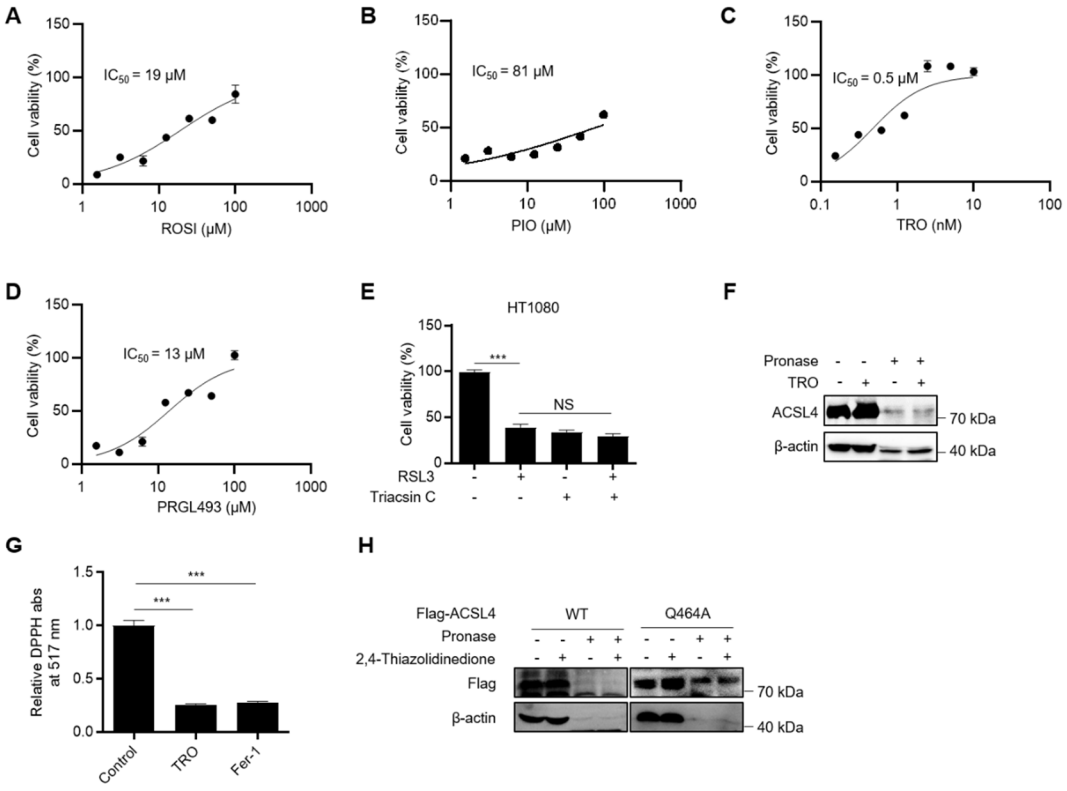

Fig. S7. **Comparison of AS with other ACSL4 inhibitors.** (A-E) Cell viability analysis of HT-1080 cells pretreated with different concentrations of ROSI (A), PIO (B), TRO (C) and PRGL493 (D) for 1 h and then stimulated with 1 μM RSL3 for 8 h. (E) Cell viability analysis of HT-1080 cells pretreated with Triacsin C for 1 h and then stimulated with 1 μM RSL3 for 8 h. (F) The cell lysates of HT-1080 was incubated with or without TRO for 2 h and then treated with different concentrations of pronase. The expression of ACSL4 was detected by immunoblotting. (G) Cell-free antioxidant potential monitored by changes in the absorbance at 517 nm of the stable radical DPPH. (H) The cell lysates of HEK293T overexpressing WT or Q464A mutant Flag-ACSL4 were incubated with or without 2,4-Thiazolidinedione for 2 h and then treated with pronase. The expression of ACSL4 was detected by immunoblotting. The concentration of all tested compounds was 50 μM. Data are the mean ± SEM. n = 3 biologically independent experiments (A-E, G). Statistical analysis was performed using an unpaired two-tailed Student's t-test. NS, $P > 0.05$, ***$P < 0.001$.

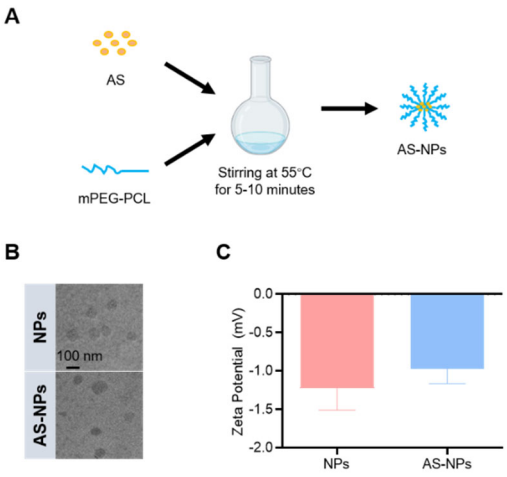

Fig. S8. **The characterization of AS-NPs.** (A) Schematic representation of the synthesis of AS-NPs. (B) The TEM images of the NPs and AS-NPs. (C) The zeta potential of the NPs and AS-NPs.

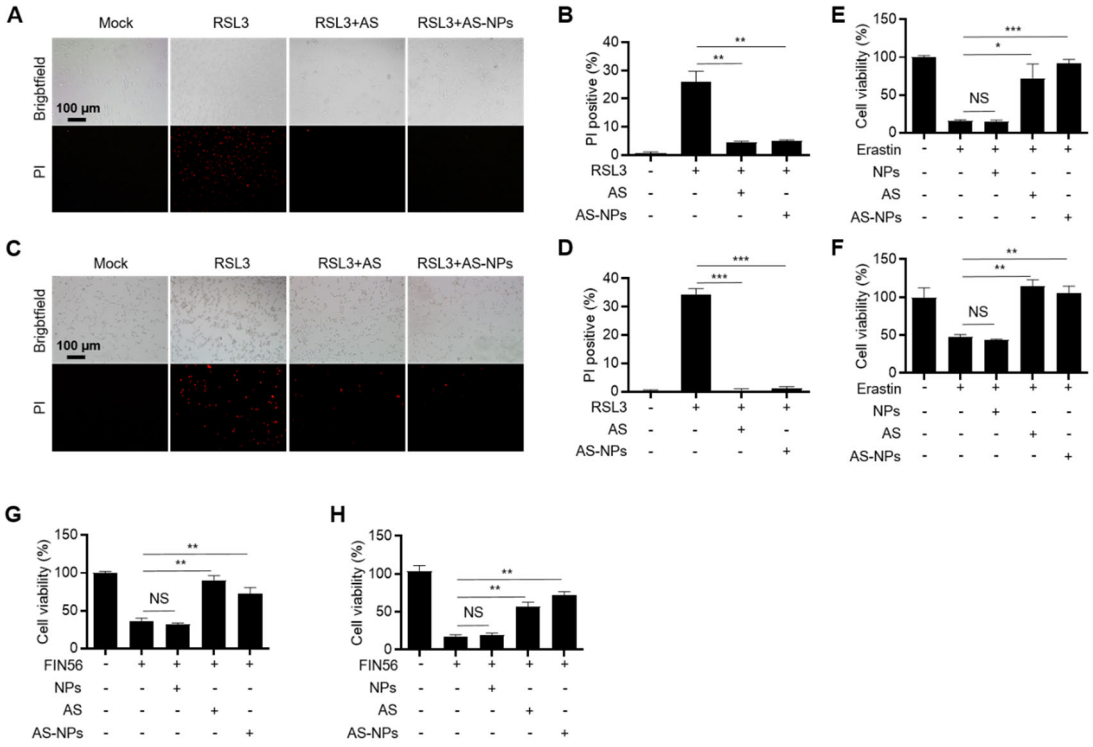

Fig. S9. AS-NPs inhibit ferroptosis induced by multiple stimuli. (A, C) Images of HT-1080 cells (A) or MDA-MB-231 cells (C) pretreated with free AS or AS-NPs for 3 h and then stimulated with 1 μM RSL3 for 8 h in the presence of propidium iodide (PI). (B, D) The percentage of PI-positive HT-1080 cells (B) or MDA-MB-231 cells (D) pretreated with free AS or AS-NPs for 3 h and then stimulated with 1 μM RSL3 for 8 h in the presence of PI. (E, F) Cell viability analysis of HT-1080 cells (E) or MDA-MB-231 cells (F) pretreated with free AS or AS-NPs for 3 h and then stimulated with 20 μM erastin for 24 h. (G, H) Cell viability analysis of HT-1080 cells (G) or MDA-MB-231 cells (H) pretreated with free AS or AS-NPs for 3 h and then stimulated with 40 μM FIN56 for 24 h. Data are the mean ± SEM. n = 3 biologically independent experiments (B, D-H). Statistical analysis was performed using an unpaired two-tailed Student's t-test. NS, $P > 0.05$, *$P < 0.05$, **$P < 0.01$, ***$P < 0.001$.

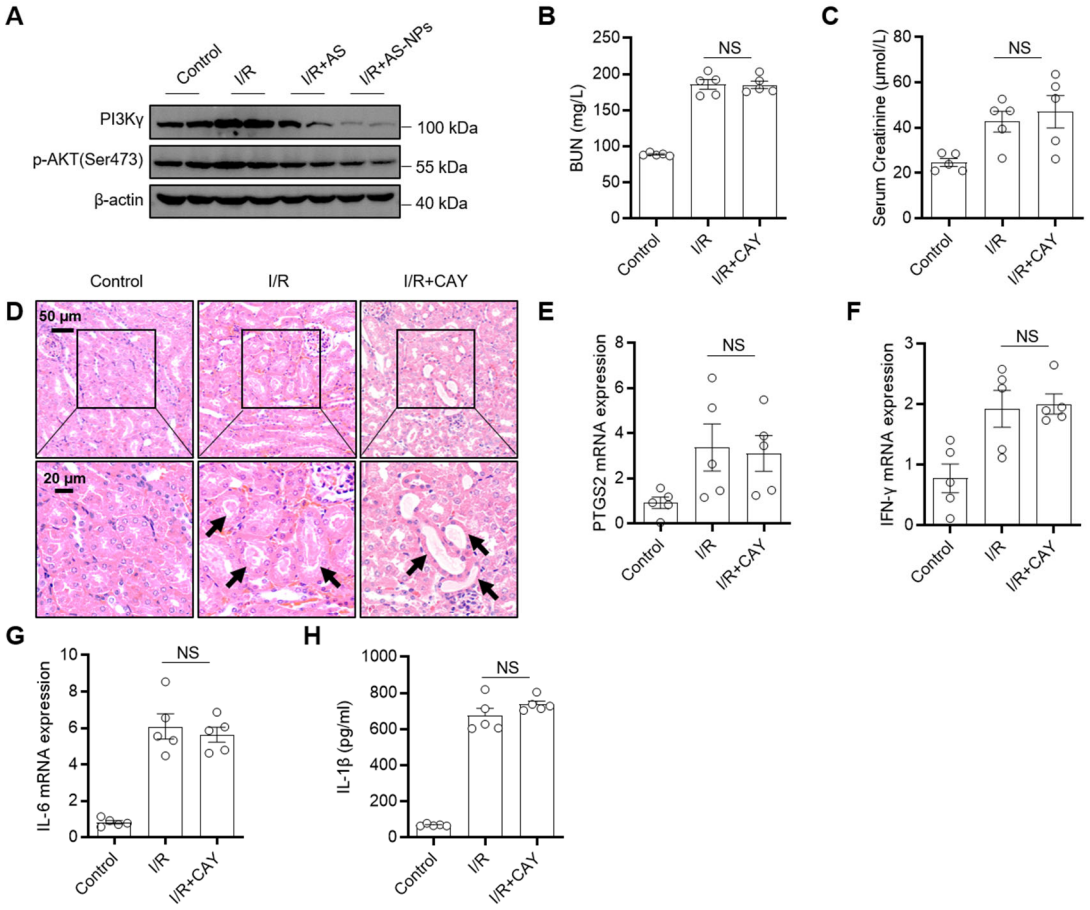

Fig. S10. CAY10505 cannot prevent the AKI. (A) Protein expression of PI3Kγ and p-AKT (Ser473) in kidney. (B) The levels of blood urea nitrogen (BUN). (C) The levels of serum creatinine. (D) Representative images of kidney sections with hematoxylin and eosin (H&E) staining. Black arrows indicate renal tubular injury during renal IRI. (E) The mRNA levels of PTGS2. (F, G) IFN-γ (F) and IL-6 (G) in kidney were evaluated by real-time PCR. (H) ELISA analysis of IL-1β in serum of C57BL/6J mice after kidney ischemia-reperfusion injury and pretreated with 20 mg/kg free AS or AS-NPs. Data are the mean ± SEM. Statistical analysis was performed using an unpaired two-tailed Student's t-test (B, C, E-H). NS, $P > 0.05$.

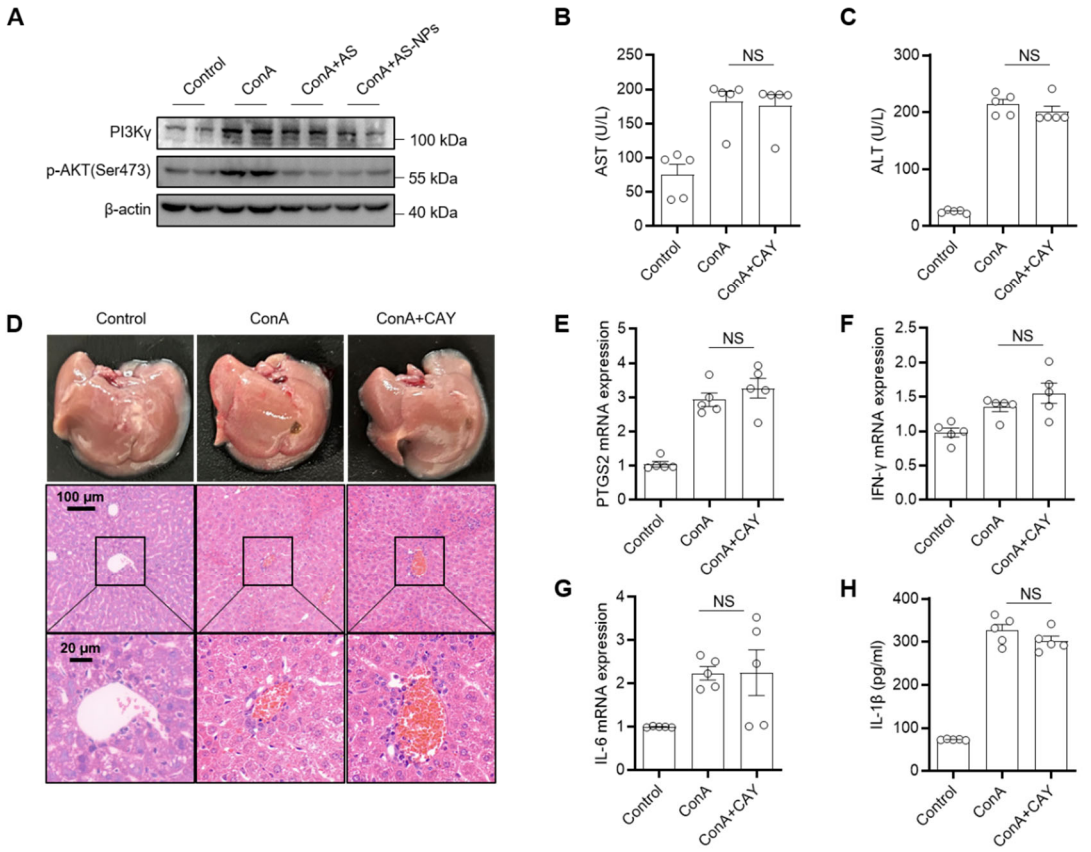

Fig. S11. CAY10505 cannot prevent the ALI. (A) Protein expression of PI3Kγ and p-AKT (Ser473) in liver. (B-H) C57BL/6J mice pretreated with 20 mg/kg free CAY or PBS and then intraperitoneally injected with 15 mg/kg ConA for 24 h. n = 5 biologically independent mice. Serum levels of AST (B) and ALT (C). Images of H&E staining in liver cross sections (D). The mRNA expression of PTGS2 (E), IFN-γ (F) and IL-6 (G) in liver were evaluated by real-time PCR. IL-1β (H) in serum were analyzed by ELISA. Data are the mean ± SEM. Statistical analysis was performed using an unpaired two-tailed Student's t-test (B, C, E-H) or generalized Wilcoxon test (A). NS, $P > 0.05$.

Table S1. Results of screening for ferroptosis inhibitors. HT-1080 cells were pretreated with inhibitors for 1 h and then stimulated with RSL3 for 8 h, cell viability was detected by CCK-8 assay.

Table S2. LC-MS/MS analysis the binding proteins of AS. HT-1080 cells treated with or without bio-AS, and then the whole cell lysate was pull-down with streptavidin beads. The precipitated proteins were separated by SDS-PAGE and stained with Coomassie blue, and then analyzed by LC-MS/MS for the binding proteins of AS.